Heliyon 6 (2020) e05874

Contents lists available at ScienceDirect

Heliyon

journal homepage: www.cell.com/heliyon

Research article

A method of purifying alpha-synuclein in *E. coli* without chromatography

Sumaer Kamboj [a], Chase Harms [a], Lokender Kumar [a], Daniel Creamer [a], Colista West [b], Judith Klein-Seetharaman [b,**], Susanta K. Sarkar [a,*]

[a] Department of Physics, Colorado School of Mines, Golden, CO 80401, USA
[b] Department of Chemistry, Colorado School of Mines, Golden, CO 80401, USA

ARTICLE INFO

Keywords:
Recombinant human alpha-synuclein
Aggregation induced by alpha-synuclein
Lewy body model system
Western blot

ABSTRACT

Research has implicated alpha-synuclein (aSyn) in pathological protein aggregation observed in almost all patients with Parkinson's disease and more than 50% of patients with Alzheimer's disease. An easy and inexpensive method of purifying aSyn and developing an *in vitro* model system of Lewy body formation would enhance basic biomedical research. We report aSyn purification technique that leverages the amyloidogenic property of aSyn suitable for purifying monomeric aSyn without chromatography and denaturing agents. We expressed full-length and untagged aSyn in Rosetta(DE3) pLysS and purified ~60 μg of aSyn from 500 mL culture within 24 h. After IPTG-induced expression of aSyn in *E. coli*, we disrupted the cells with a sonicator. We centrifuged the cell lysate in a 15 mL tube, which leads to aSyn-induced aggregation of native *E. coli* proteins. After removing aggregates, centrifugation in a 30 kDa cut-off filter followed by a 10 kDa cut-off filter led to purified water-soluble aSyn. The identity of aSyn was confirmed by Western blot using anti-aSyn antibody and Edman sequencing. Its mass was determined to be 14.6 kDa using a MALDI TOF-MS mass spectrometer. The majority of aSyn led to water-suspended (as opposed to precipitated) aggregation of *E. coli* proteins with visible fibrous structures. The broad-spectrum binding and amyloidogenic property of aSyn is thus not only useful for inexpensive aSyn production for diverse applications, but it also expands studying its possible roles in human physiology. The aggregate of *E. coli* proteins induced by aSyn during the purification process may serve as a Lewy body model.

1. Introduction

Alzheimer's disease (AD) and Parkinson's disease (PD) are the leading causes of neurodegeneration in the older population. 5.8 million patients are currently living with AD in the US [1]. This number includes an estimated 5.6 million people age 65 and older and approximately 200,000 individuals under the age of 65 who have early-onset AD, which may double by 2025 with a projected total cost of care of more than $1 trillion per year in 2050. Also, ~1 million patients already have PD in the US [2], and ~60,000 new cases per year appear in the US, with a total cost of care estimated to be ~$52 billion per year. More than 50% of patients with AD and almost all patients with PD [3] show Lewy bodies, intraneuronal cytoplasmic protein aggregates. The typical protein in Lewy bodies that may be causally related to the etiology of AD and PD is alpha-synuclein (aSyn) [4].

The physiological functions of aSyn remain unclear, but its primary localization in the cytoplasm of mainly neuronal cells [5,6,7] and at presynaptic terminals [5,8,9,10] implies a role in neuronal function. Also, aSyn is associated with the distal reserve pool of synaptic vesicles [7,11,12]. An overexpression [13,14] or knock out [15,16,17] of aSyn leads to dysregulation of synaptic transmission. These studies suggest that aSyn plays an essential role in regulating neurotransmitter release and synaptic function [18]. A growing body of evidence from *in vitro* and *in vivo* genetic, biochemical, and biophysical studies suggest that aSyn oligomerization [19,20] and fibrillation [21,22] play a central role in Lewy body pathologies, including AD and PD. There is evidence that the C-terminal truncation of aSyn by proteases leads to protein aggregation and Lewy body formation. Research has shown that asparaginyl endopeptidase (AEP) [23] causes partial cleavage of aSyn. A growing body of evidence suggests that matrix metalloproteases can also partially cleave aSyn [24,25,26,27,28]. However, the mechanisms and cellular pathways leading to neurodegeneration caused by aSyn-induced aggregation remain unknown despite many biophysical studies [29,30,31]. Addressing these knowledge gaps will require further biophysical and

* Corresponding author.
** Corresponding author.
E-mail addresses: judithks@mines.edu (J. Klein-Seetharaman), ssarkar@mines.edu (S.K. Sarkar).

https://doi.org/10.1016/j.heliyon.2020.e05874
Received 15 February 2020; Received in revised form 18 February 2020; Accepted 24 December 2020

biochemical studies of the mechanisms underlying protein aggregation induced by aSyn [32], which in turn would require purified aSyn as well as a model of protein aggregates.

Since the first identification of synucleins in the human brain and *E. coli* based purification of recombinant synucleins in 1994 [9], several reports of recombinant purification have been reported for aSyn [33,34,35,36]. Protein purification usually requires time-consuming and expensive steps of chromatography to separate proteins of interest from other proteins. Generally, cell lysate goes through a series of purification steps such as precipitation by ammonium sulfate or acid, ion exchange, and size exclusion chromatography [37]. For higher specificity, several fusion strategies such as the glutathione S-transferase (GST) system [38] and the chitin-binding domain/intein system [39] are also useful. Leveraging periplasmic localization of expressed aSyn in *E. coli*, a shorter purification protocol was developed [40]. For NMR studies, isotopically labeled aSyn was purified in *E. coli* [41]. For the delivery of aSyn inside cells, researchers have purified Tat-fused recombinant aSyn in *E. coli* [42]. For purifying aSyn with post-translational modifications, Gerding et al. reported a method of purifying aSyn with 3-nitrotyrosine in *E. coli* [43]. These methods can provide good purity and homogeneity of purified aSyn within three or more days. Recombinant aSyn purified in *E. coli* has enabled many *in vitro* and even *in vivo* studies revealing many insights into structure-function relationships of aSyn. Based on these studies using recombinant protein, aSyn is generally considered a "natively unfolded" ~14.6 kDa monomer [35] that can form secondary α-helical structures upon binding to lipid membranes and detergents [44].

In contrast to the monomeric form of recombinant protein, aSyn purified from the human brain [45], live human cells, neuronal and non-neuronal cell lines predominantly show a "natively folded" ~58 kDa tetrameric form [46]. The additional efforts to purify aSyn destabilize the tetrameric forms, leading to the monomeric form [45]. Several factors affect aSyn studies, including purification [37,45], denaturing step, high concentration, and post-translational modification [47]. To enable further studies of the structure-function relationships of aSyn, we developed a quick and inexpensive method of aSyn purification in *E. coli*. We describe a method to purify untagged recombinant aSyn within 24 h, where we have eliminated chromatography from aSyn purification by exploiting the propensity of aSyn to form aggregates. Our core technology involves "self-purification" of aSyn, which is possible because aSyn leads to aggregation of *E. coli* proteins leaving soluble full-length aSyn. As a result, we obtained purified aSyn and a model of aSyn-induced protein aggregates to enable further biochemical and biophysical studies.

2. Results and discussion

2.1. aSyn is toxic for E. coli

We expressed full-length recombinant human aSyn with 140 residues in *E. coli*. The molecular weight of full-length aSyn is ~14.5 kDa. We inserted the sequence of aSyn into the pET11a vector between NdeI (N-terminal) and HindIII (C-terminal) restriction sites. We transformed the plasmid into Rosetta (DE3) pLysS competent *E. coli* strain for aSyn expression. The aSyn in the plasmid is under the control of the lac operator, and as such, we induced aSyn expression using 1 mM Isopropyl β-d-1-thiogalactopyranoside (IPTG) at Optical Density (OD_{600}) = 0.17. As shown in Figure 1a, IPTG-induced production of aSyn inhibited *E. coli* growth. However, *E. coli* growth was unaffected for 2.5 h after IPTG induction, indicating a threshold concentration of intracellular aSyn for toxicity. We used Congo red, a stain for amyloid [49,50], to test if aSyn production after IPTG induction leads to amyloid formation. *E. coli* culture without IPTG induction served as the control. We incubated cultures with and without IPTG induction at the same OD, centrifuged and

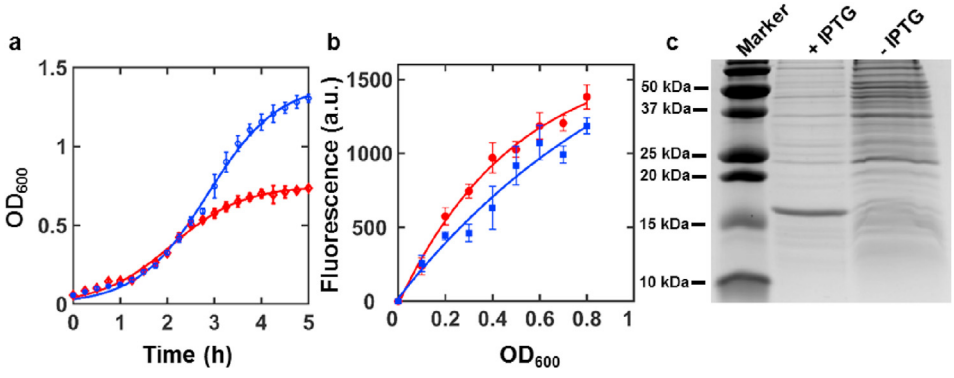

Figure 1. Expression of aSyn in *E. coli*. (a) Growth of *E. coli* strain Rosetta(DE3) pLysS with (red diamond) and without (blue circle) IPTG. The data are fitted to the logistic equation for bacterial growth, $a/[1+b\exp(-kt/60)]$, with (solid red line) and without (solid blue line); the best-fit parameters are $a = 0.8 \pm 0.1$ (with IPTG), 1.5 ± 0.3 (without IPTG); $b = 15 \pm 22$(with IPTG), 24 ± 26 (without IPTG); $k = 1.3 \pm 0.7$ (with IPTG), 1.0 ± 0.5 (without IPTG). The error bars represent standard deviations of three replicates. Induction by IPTG produces aSyn, which is toxic for *E. coli*, as indicated by the reduced growth in the presence of IPTG. (b) Fluorescence from Congo red stain between 565 nm and 650 nm with (solid red circle) and without (solid blue circle) IPTG upon excitation at 470 nm. The data are fitted to the equation, $d - e \times \exp(-f \times x)$, with (solid red line) and without (solid blue line); the best-fit parameters are $d = 1680 \pm 178$ (with IPTG), 2263 ± 1479 (without IPTG); $e = 1699 \pm 161$ (with IPTG), 2243 ± 1430 (without IPTG); $f = 2.01 \pm 0.42$ (with IPTG), 0.91 ± 0.52 (without IPTG). The error bars represent standard deviations of four replicates. (c) Expression of aSyn with and without IPTG. A comparison of protein expression with and without IPTG showed a band at ~16 kDa due to aSyn, which is higher than the actual mass. Published reports have shown aSyn indicating a little higher weight in SDS PAGE [26,40,41,48] and expected value in SDS PAGE [27]. See the supplementary information (Fig. S2) for SDS PAGE, showing both higher and expected molecular weights depending on the experimental conditions. For full gel, see Fig. S3a.

discarded supernatant, reconstituted the cells in water, and measured Congo red fluorescence (see methods for detailed procedure). Figure 1b shows that Congo red fluorescence with IPTG induction is higher than without IPTG induction at each OD, suggesting that aSyn forms amyloid inside *E. coli* and reduces growth observed in Figure 1a. The supernatant of centrifuged cell lysates was analyzed using SDS PAGE, as shown in Figure 1c, which showed a band at ~15 kDa due to aSyn after induction with IPTG. As a negative control, cells without IPTG induction did not produce aSyn. A comparison of protein bands with and without IPTG revealed that *E. coli* protein bands were of lighter intensity when aSyn was present. In combination with the reduced growth (Figure 1a), this observation suggests that aSyn leads to aggregation of *E. coli* proteins and causes toxicity.

2.2. aSyn leads to water-suspended structures and forms oligomers upon centrifugation

We observed that the centrifugation of *E. coli* lysate at 10000 rpm in a 15 mL tube led to water-suspended structures that did not precipitate (Figure 2a). The water-suspended structures revealed different morphologies under a light microscope (Figure 2b). The soluble portion in Figure 2a showed oligomers in Western blot (WB) imaging (Figure 2c). The soluble part's centrifugation using a 30 kDa filter led to further aggregation and a clear flow through (Figure 2d). Interestingly, the water-suspended structures did not form in a 50 mL tube, suggesting that centrifugal force in combination with narrow diameters leads to the water-suspended aggregation.

2.3. Aggregation of E. coli proteins induced by aSyn facilitates purification

We leveraged the aggregation of *E. coli* proteins to purify aSyn without chromatography using 30 kDa and 10 kDa centrifugation filters (Figure 3a). The identity of aSyn was confirmed by WB using an anti-aSyn antibody (Figure 3b). We used the Bradford assay to quantify the concentration of purified aSyn. Figure 3c shows the standard curve generated using bovine serum albumin (BSA), where the red symbol indicates the data point due to aSyn. We obtained ~60 μg of purified aSyn in solution from 500 mL culture within 24 h. Note that we got a lower amount of purified aSyn because we also formed aggregates of native *E. coli* proteins leveraging the amyloidogenic property of aSyn.Also, we performed mass spectrometry and Edman sequencing of purified aSyn at the Tufts Core Facility. Mass spectrometry (Figure 3d) confirmed that the purified aSyn did not have higher molecular weight contamination. Further, Edman sequencing confirmed the first seven amino acids to be MDVFMKG as expected (see Fig. S1).

In conclusion, we have developed an inexpensive and quick method of purifying ~60 µg recombinant aSyn in *E. coli* within 24 h Figure 4 shows the purification flowchart. Two critical steps are the use of sonication and narrow diameter tubes for centrifugation. We compared purified aSyn with commercially available aSyn (Fig. S2), which shows comparable purity. In the future, functional studies such as fibrillation kinetics are needed to compare the two sources of aSyn. In contrast to the chromatography-free method in this paper, chromatography-based purification techniques using denaturing agents take a few days. Recently, Gerding et al. reported a process of purifying ~1 mg of aSyn in *E. coli* [43] involving two chromatographic steps. Although 60 µg of aSyn from 500 mL of *E. coli* culture in our paper is significantly less than ~1 mg of aSyn, aSyn-induced protein aggregates are an important byproduct of the method described in this paper. The formation of aggregates enables chromatography-free purification but leads to the lower yield of purified aSyn. These aggregates might be useful as a model of Lewy bodies. However, further studies are needed to confirm whether or not these aggregates can be used as a model of Lewy bodies. The production of aSyn-induced aggregates, in addition to purified monomeric aSyn, is unique relative to the prior reports on aSyn purification. We have observed oligomers of aSyn in the supernatant, as suggested by WB (Figure 2c), before purifying monomeric aSyn (Figure 3a). The observation of aSyn oligomers is consistent with previous reports of the tetrameric form of aSyn [45,46]. However, we cannot conclude the precise stoichiometry because we did not perform any size exclusion chromatography in our chromatography-free method. The dramatic substrate promiscuity of aSyn enables purification and affects *E. coli* growth (Figure 1a). We used Congo red [49,50] to detect amyloid formation in *E. coli* (Figure 1b). In the future, we need functional data to define the toxicity of purified aSyn in mammalian cells and animal models. To this end, thioflavin T (ThT) [51] and 1-anilinonaphthalene-8-sulfonic acid (ANS) [52] may provide additional information about fibrillation. Both ThT and ANS emit enhanced fluorescence upon binding fibrils. However, ThT emits stronger fluorescence upon binding the β-sheet conformation of amyloid fibrils. In contrast, ANS emits enhanced fluorescence upon attaching to hydrophobic surfaces. As such, ANS is a suitable probe for partially unfolded protein conformations. The promiscuity of aSyn with *E. coli* proteins suggests that aSyn may have more physiological implications than neurodegeneration.

3. Materials and methods

3.1. Transformation of the plasmid

The plasmid contains the DNA sequence for 140-residue wild type aSyn inserted into the pET11a vector between NdeI (N-terminal) and HindIII (C-terminal) restriction sites. We transformed the plasmid into Rosetta (DE3) pLysS *E. coli* (Millipore, Cat# 70956-4). We thawed 50 µL of cells on ice. 10 µL of plasmid at 100 ng/mL concentration was added to

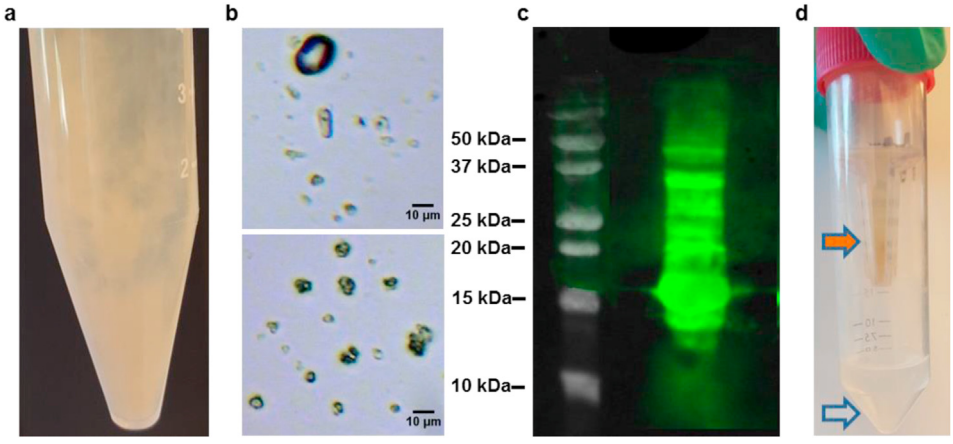

Figure 2. Aggregation of aSyn. (a) Water-insoluble but suspended aggregates of *E. coli* proteins induced by aSyn. (b) Examples of structures observed under a light microscope. (c) WB of the soluble proteins in Figure 2a shows oligomers of aSyn. A calorimetric image (gray bands on the left) of the molecular weight markers superimposed with the WB image. (d) Centrifugation of the soluble proteins in Figure 2a using a 30 kDa cut-off filter leads to further aggregation (orange arrow) and a clear flow-through (gray arrow). Filtration of the flow-through using a 10 kDa cut-off centrifugation filter gives purified aSyn. For full WB, see Fig. S3b.

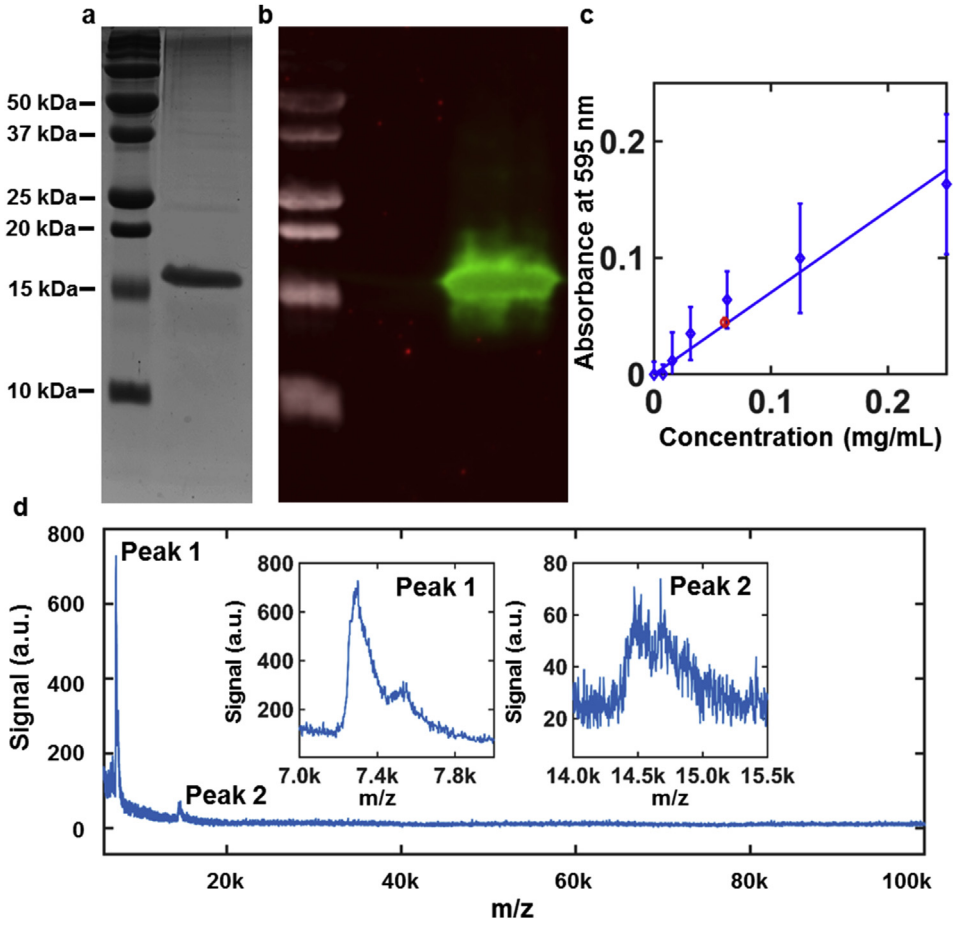

Figure 3. Purification, quantification, and identification of aSyn. (a) Purified aSyn. Left lane: molecular weight marker; right lane: aSyn. (b) WB using an anti-aSyn antibody. A calorimetric image (gray bands on the left) of the markers superimposed with the WB image. (c) Bradford standard curve generated using BSA as the standard. The solid line is the best fit to a line $y = ax$; the best-fit parameter is $a = 0.7 \pm 0.1$ (standard deviation of three replicates). The red square due to aSyn results in a concentration of ~60 μg/mL (d) MALDI-TOF mass spectrum of aSyn shows the purity of aSyn. Two peaks appear due to aSyn: peak 1 (7.3 kDa and 7.5 kDa) and peak 2 (14.5 kDa and 14.7 kDa). For full gel and WB, see Fig. S3c-d.

the cells and kept on ice for 30 min. We transferred cells to a hot water bath at 42 °C for 45 s and moved back to the ice for 5 min. 950 μL of super optimal broth with catabolite repression (SOC) media (Sigma-Aldrich, Cat# S1797) was added to the cells and incubated for 2 h at 37 °C. We spread 100 μL of growth on a plate containing ImMedia Amp Blue (Invitrogen, Cat# 45-0038) and allowed to grow for 48 h. After 48 h, we selected one colony of *E.coli* and transferred into 35 mL of Luria Broth (LB) media with 35 μL of ampicillin at 100 mg/mL concentration and 35 μL of chloramphenicol at 34 mg/mL concentration. Cells were grown for an additional 16 h until OD_{600} reached 1.5. To make glycerol stock, we added 800 μL of *E. coli* culture to 500 μL of 50% glycerol (Sigma-Aldrich, Cat# G5516) and stored in -80 °C.

3.2. Growth of Rosetta (DE3) pLysS cells

We prepared 35 mL of seed culture in LB media (Sigma-Aldrich L7658) from 3 mL of *E. coli* cells' glycerol stocks. We added 35 μL of ampicillin at 100 mg/mL concentration and 35 μL of chloramphenicol at 34 mg/mL concentration. The seed culture was grown overnight for 15 h in shaker-incubator at 37 °C with 250 rpm orbital agitation until growth reached $OD_{600} = 1.8$. 10 mL of the seed culture was added to 500 mL sterile LB media with the same final concentrations of antibiotics in two 1 L conical flat-bottom glass flasks and grown at 37 °C with 250 rpm orbital agitation. After the growth reached $OD_{600} = 0.2$, we induced the cells in one flask with 500 μL of 1 M IPTG (ChemCruz, Cat# SC-202185B). The cells in the other flask were not induced with IPTG to serve as the negative control. After induction, we grew cells in both flasks for 5 h in the incubator-shaker at 37 °C with 250 rpm orbital agitation. We measured OD using a cell density meter (WPA Biowave, Model# C0800) to quantify the growth, as shown in Figure 1a. The cells were harvested and centrifuged in 15 mL centrifuge tubes at 10000 rpm for 10 min using a fixed angle centrifuge (Sorvall Lynx 4000 centrifuge with F12-6X500 rotor, Cat# 75006580). Note that LB media was sterilized by an autoclave (Panasonic, Model# MLS-3781L) following the preset liquid sterilization program (121 °C for 15 min).

3.3. Congo red staining

We collected 1 mL of culture from 500 mL stock cultures with and without IPTG at $OD_{600} = 0.1$, 0.2, 0.3, 0.4, 0.5, 0.6, 0.7, and 0.8. We centrifuged the 1 mL cultures in 1.5 mL microcentrifuge tubes at 10,000 rpm for 10 min. After discarding the supernatant, we added 200 μL of Congo Red stain (Abcam, Cat# ab150663) to each sample tube and vortexed briefly to reconstitute cells. We incubated the cells with Congo red at 37 °C for 10 min. After centrifugation of samples at 10,000 rpm for 10 min, we removed the excess stain and added 500 uL of deionized water to reconstitute the stained *E. coli* by brief vortexing. We loaded 200 μL of each sample into thin-walled PCR tubes and measured the Congo red emission in the range of 565–650 nm using a DeNovix Fluorometer QFX with 470 nm excitation (Figure 1b).

3.4. Cell lysis and SDS PAGE to confirm the expression of aSyn

We took 10 mL of each growth and disrupted the cells using a sonicator (Branson Digital Sonifier, Model# BBT16031593A) at 30% amplitude for 10 min with a sequence of 10 s pulse ON and 20 s pulse OFF. We centrifuged the cell lysates and collected the supernatant containing soluble proteins. These samples were prepared for SDS PAGE by 1:1 dilution in sample buffer with β-mercaptoethanol (Sigma-Aldrich, Cat# M3148) made from 2x Laemmli buffer (Biorad, Cat# 161–0737).

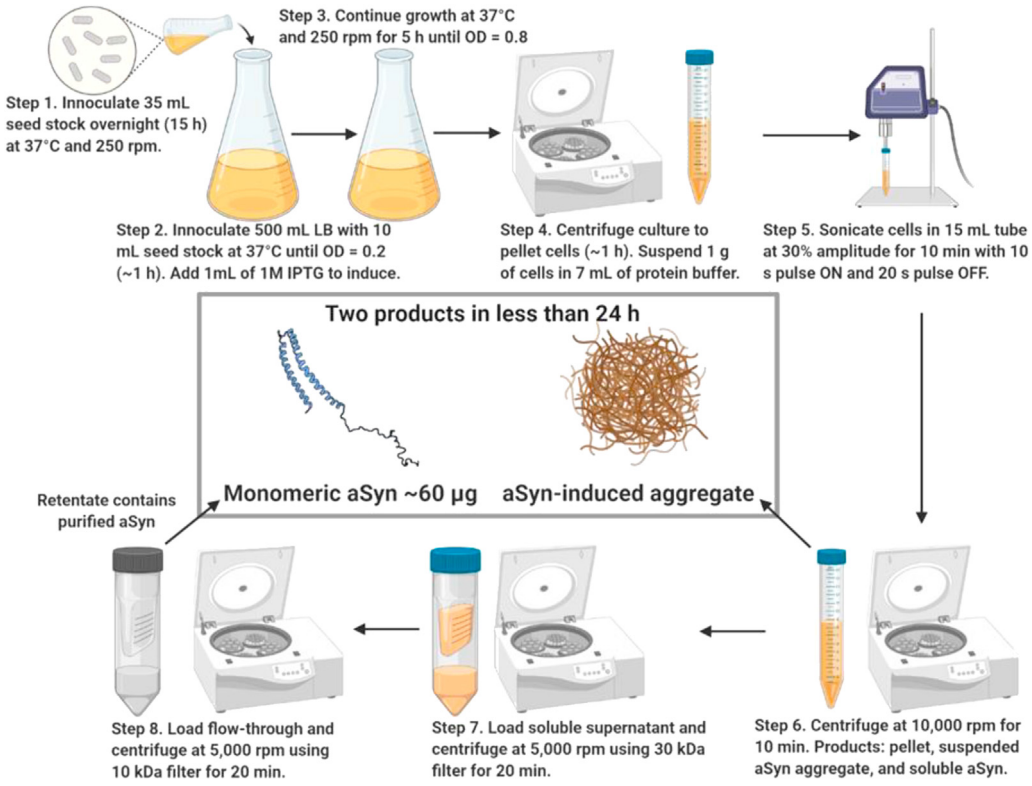

Figure 4. Flowchart of aSyn purification in *E. coli*. In less than 24 h, it is possible to purify 60 µg of monomeric aSyn from 500 mL of *E. coli* culture and obtain aSyn-induced aggregates. The use of sonication in Step 5 and narrow diameter tubes (15 mL) for centrifugation in Step 6 are essential for optimum results. Created with BioRender.com.

We boiled the samples with the dye for 10 min and loaded 30 µL of each sample into the wells of a 15% polyacrylamide gel. The gel was run in 1X SDS running buffer at 70 V and 40 mA. After 30 min, we increased the voltage to 120 V and allowed the gel to run for an additional 1 h. Gels were removed from the running tank and stained in 100 mL of stain prepared using 30% ethanol, 10% acetic acid, and 0.5% Coomassie Brilliant Blue R-250 (Biorad, Cat# 161–0436). The gel was stained for 2 h and washed twice in DI water to remove excess dye, followed by destaining in 200 mL of 30% ethanol and 10% acetic acid for 18 h. We imaged the gel using an imager (Figure 1c).

3.5. Protein aggregation induced by centrifugation of high aSyn concentration in narrow tubes

We caused protein aggregation by aSyn as an integral part of our purification to pull down native *E.coli* proteins, and aSyn effectively self-purified itself. We reconstituted 1 g cell pellet in 6 mL of protein buffer (50 mM Tris, 100 mM NaCl, pH 9.0) in a 15 mL tube and disrupted the cells using a sonicator as described before. The step of lysate centrifugation in a 15 mL tube at 10000 rpm for 10 min is critical. After centrifugation, we observed water-suspended structures. Note that the water-suspended structures did not form when we centrifuged the cell lysate in a 50 mL tube. We also noted that even with longer centrifugation, the water-suspended structures did not precipitate and form a pellet at the bottom of the tube and remained suspended in solution. The suspended insoluble structures were highly viscous and cohesive, like mucus. We could pull out the structures from the solution using a 1 mL pipet tip. The soluble supernatant was filtered using a 30 kDa Amicon filter tube (Millipore, Cat# UFC903024) at 5000 rpm for 20 min. The flow-through of filtration was then loaded into a 10 kDa Amicon filter tube (Millipore, Cat# ACS501012) and centrifuged at 5000 rpm for 20 min. The retentate from this filtration contained purified aSyn, which we checked using a 15% SDS PAGE. The gel was run at 150 V for 10 min and then 200 V for 45 min. After purification, we obtained 1 mL of ~60 µg/mL aSyn. We quantified the protein concentration using the Bradford assay (Figure 3c).

3.6. Identification of aSyn using Western blotting

We ran the SDS PAGE of the protein sample in 15% polyacrylamide gel as before. Then, we transferred the proteins to a nitrocellulose membrane using the Trans-Blot Turbo transfer system (Biorad, Model# 170–4155). Then, we dipped the membrane with transferred proteins into 30 mL of blocking buffer (skim milk) and placed on a shaker for 2 h. After removing the blocking buffer, we added the primary anti-aSyn antibody (Abcam, Cat# 138501) to a final concentration of 0.5 μg/mL in 10 ml of blocking buffer and placed on a shaker at 4 °C for 16 h. After removing the primary antibody solution, we washed the blot 3 times with 30 mL of protein buffer (50 mM Tris, 100 mM NaCl, pH 9.0). After washing, we dipped the membrane into 50 mL of the secondary antibody (Bosterbio, Cat# BA1054) at a final concentration of 0.5 μg/mL for 2 h. We removed the secondary antibody solution and rewashed the blot with 30 mL of protein buffer. 12 ml of the chemiluminescent substrate (Biorad, Clarity Western ECL substrate, Cat# 170–5060) was added to the blot and imaged using a Biorad imager.

3.7. Identification and quantification of aSyn

In addition to WB, we confirmed the identity of purified aSyn using mass spectroscopy and Edman sequencing performed by the Tufts Core Facility at Tufts Medical School. To quantify aSyn concentration, we used Pierce Detergent Compatible Bradford Assay Kit (Thermo Scientific, Cat# 23246). We created a standard curve using BSA with known concentrations in protein buffer (100 mM NaCl, 50 mM Tris, pH 9.0). We measured the absorbance at 595 nm and subtracted the blank reading without BSA from the absorbance measurements. We fitted the standard curve to a

linear model and quantified the aSyn concentration from the best-fit parameters.

Declarations

Author contribution statement

Sumaer Kamboj, Chase Harms, Lokender Kumar & Colista West: Performed the experiments; Analyzed and interpreted the data.

Daniel Creamer: Performed the experiments.

Judith Klein-Seetharaman: Conceived and designed the experiments; Analyzed and interpreted the data.

Susanta K. Sarkar: Developed the purification scheme; Conceived and designed the experiments; Analyzed and interpreted the data; Wrote the paper.

Funding statement

One grant to S.K.S. and J.K.S. from the National Institutes of Health (RGM137295A) partially supported this work.

Data availability statement

Data included in article/supp. material/referenced in article.

Declaration of interests statement

Patent pending.

Additional information

Supplementary content related to this article has been published online at https://doi.org/10.1016/j.heliyon.2020.e05874.

Acknowledgements

The authors would like to acknowledge Dr. Narinder Sanghera for providing the plasmid for aSyn.

References

[1] Alzheimer's Association, Alzheimer's disease facts and figures, Alzheimer's & Dementia 13 (2017) 325–373, 2017.
[2] C. Marras, J. Beck, J. Bower, E. Roberts, B. Ritz, G. Ross, R. Abbott, R. Savica, S. Van Den Eeden, A. Willis, Prevalence of Parkinson's disease across North America, NPJ Parkinson's disease 4 (2018) 21.
[3] L. Parkkinen, T. Pirttilä, I. Alafuzoff, Applicability of current staging/categorization of α-synuclein pathology and their clinical relevance, Acta Neuropathol. 115 (2008) 399–407.
[4] M.G. Spillantini, M.L. Schmidt, V.M.-Y. Lee, J.Q. Trojanowski, R. Jakes, M. Goedert, α-Synuclein in Lewy bodies, Nature 388 (1997) 839.
[5] J.M. George, H. Jin, W.S. Woods, D.F. Clayton, Characterization of a novel protein regulated during the critical period for song learning in the zebra finch, Neuron 15 (1995) 361–372.
[6] U. Dettmer, A.J. Newman, E.S. Luth, T. Bartels, D. Selkoe, In vivo cross-linking reveals principally oligomeric forms of α-synuclein and β-synuclein in neurons and non-neural cells, J. Biol. Chem. 288 (2013) 6371–6385.
[7] P.J. Kahle, M. Neumann, L. Ozmen, V. Müller, H. Jacobsen, A. Schindzielorz, M. Okochi, U. Leimer, H. van der Putten, A. Probst, Subcellular localization of wild-type and Parkinson's disease-associated mutant α-synuclein in human and transgenic mouse brain, J. Neurosci. 20 (2000) 6365–6373.
[8] A. Iwai, E. Masliah, M. Yoshimoto, N. Ge, L. Flanagan, H.R. De Silva, A. Kittel, T. Saitoh, The precursor protein of non-Aβ component of Alzheimer's disease amyloid is a presynaptic protein of the central nervous system, Neuron 14 (1995) 467–475.
[9] R. Jakes, M.G. Spillantini, M. Goedert, Identification of two distinct synucleins from human brain, FEBS Lett. 345 (1994) 27–32.
[10] G.S. Withers, J.M. George, G.A. Banker, D.F. Clayton, Delayed localization of synelfin (synuclein, NACP) to presynaptic terminals in cultured rat hippocampal neurons, Dev. Brain Res. 99 (1997) 87–94.
[11] S. Lee, H. Jeon, K.V. Kandror, Alpha-synuclein is localized in a subpopulation of rat brain synaptic vesicles, Acta Neurobiol. Exp. 68 (2008) 509–515.
[12] L. Zhang, C. Zhang, Y. Zhu, Q. Cai, P. Chan, K. Uéda, S. Yu, H. Yang, Semi-quantitative analysis of α-synuclein in subcellular pools of rat brain neurons: an immunogold electron microscopic study using a C-terminal specific monoclonal antibody, Brain Res. 1244 (2008) 40–52.
[13] K.E. Larsen, Y. Schmitz, M.D. Troyer, E. Mosharov, P. Dietrich, A.Z. Quazi, M. Savalle, V. Nemani, F.A. Chaudhry, R.H. Edwards, α-Synuclein overexpression in PC12 and chromaffin cells impairs catecholamine release by interfering with a late step in exocytosis, J. Neurosci. 26 (2006) 11915–11922.
[14] V.M. Nemani, W. Lu, V. Berge, K. Nakamura, B. Onoa, M.K. Lee, F.A. Chaudhry, R.A. Nicoll, R.H. Edwards, Increased expression of α-synuclein reduces neurotransmitter release by inhibiting synaptic vesicle reclustering after endocytosis, Neuron 65 (2010) 66–79.
[15] A. Abeliovich, Y. Schmitz, I. Fariñas, D. Choi-Lundberg, W.-H. Ho, P.E. Castillo, N. Shinsky, J.M.G. Verdugo, M. Armanini, A. Ryan, Mice lacking α-synuclein display functional deficits in the nigrostriatal dopamine system, Neuron 25 (2000) 239–252.
[16] L. Yavich, H. Tanila, S. Vepsäläinen, P. Jäkälä, Role of α-synuclein in presynaptic dopamine recruitment, J. Neurosci. 24 (2004) 11165–11170.
[17] L. Yavich, P. Jäkälä, H. Tanila, Abnormal compartmentalization of norepinephrine in mouse dentate gyrus in α-synuclein knockout and A30P transgenic mice, J. Neurochem. 99 (2006) 724–732.
[18] F. Cheng, G. Vivacqua, S. Yu, The role of alpha-synuclein in neurotransmission and synaptic plasticity, J. Chem. Neuroanat. 42 (2011) 242–248.
[19] K.A. Conway, J.D. Harper, P.T. Lansbury, Accelerated in vitro fibril formation by a mutant α-synuclein linked to early-onset Parkinson disease, Nat. Med. 4 (1998) 1318.
[20] I.F. Tsigelny, L. Crews, P. Desplats, G.M. Shaked, Y. Sharikov, H. Mizuno, B. Spencer, E. Rockenstein, M. Trejo, O. Platoshyn, Mechanisms of hybrid oligomer formation in the pathogenesis of combined Alzheimer's and Parkinson's diseases, PloS One 3 (2008) e3135.
[21] A. Oueslati, M. Fournier, H.A. Lashuel, Role of post-translational Modifications in Modulating the Structure, Function and Toxicity of α-synuclein: Implications for Parkinson's Disease Pathogenesis and Therapies, Progress in Brain Research, Elsevier, 2010, pp. 115–145.
[22] G. Taschenberger, M. Garrido, Y. Tereshchenko, M. Bähr, M. Zweckstetter, S. Kügler, Aggregation of αSynuclein promotes progressive in vivo neurotoxicity in adult rat dopaminergic neurons, Acta Neuropathol. 123 (2012) 671–683.
[23] Z. Zhang, S.S. Kang, X. Liu, E.H. Ahn, Z. Zhang, L. He, P.M. Iuvone, D.M. Duong, N.T. Seyfried, M.J. Benskey, Asparagine endopeptidase cleaves α-synuclein and mediates pathologic activities in Parkinson's disease, Nat. Struct. Mol. Biol. 24 (2017) 632.
[24] H. Mizoguchi, K. Yamada, T. Nabeshima, Matrix metalloproteinases contribute to neuronal dysfunction in animal models of drug dependence, Alzheimer's disease, and epilepsy, Biochemistry research international 2011 (2011).
[25] A. Leake, C. Morris, J. Whateley, Brain matrix metalloproteinase 1 levels are elevated in Alzheimer's disease, Neurosci. Lett. 291 (2000) 201–203.
[26] J. Levin, A. Giese, K. Boetzel, L. Israel, T. Högen, G. Nübling, H. Kretzschmar, S. Lorenzl, Increased α-synuclein aggregation following limited cleavage by certain matrix metalloproteinases, Exp. Neurol. 215 (2009) 201–208.
[27] J.Y. Sung, S.M. Park, C.-H. Lee, J.W. Um, H.J. Lee, J. Kim, Y.J. Oh, S.-T. Lee, S.R. Paik, K.C. Chung, Proteolytic cleavage of extracellular secreted α-synuclein via matrix metalloproteinases, J. Biol. Chem. 280 (2005) 25216–25224.
[28] G.A. Rosenberg, Matrix metalloproteinases and their multiple roles in neurodegenerative diseases, Lancet Neurol. 8 (2009) 205–216.
[29] M.M. Dedmon, K. Lindorff-Larsen, J. Christodoulou, M. Vendruscolo, C.M. Dobson, Mapping long-range interactions in α-synuclein using spin-label NMR and ensemble molecular dynamics simulations, J. Am. Chem. Soc. 127 (2005) 476–477.
[30] V.N. Uversky, J. Li, P. Souillac, I.S. Millett, S. Doniach, R. Jakes, M. Goedert, A.L. Fink, Biophysical properties of the synucleins and their propensities to fibrillate inhibition of α-synuclein assembly by β-and γ-synucleins, J. Biol. Chem. 277 (2002) 11970–11978.
[31] C.M. Pfefferkorn, Z. Jiang, J.C. Lee, Biophysics of α-synuclein membrane interactions, Biochim. Biophys. Acta Biomembr. 1818 (2012) 162–171.
[32] H.A. Lashuel, C.R. Overk, A. Oueslati, E. Masliah, The many faces of α-synuclein: from structure and toxicity to therapeutic target, Nat. Rev. Neurosci. 14 (2013) 38.
[33] B.I. Giasson, K. Uryu, J.Q. Trojanowski, V.M.-Y. Lee, Mutant and wild type human α-synucleins assemble into elongated filaments with distinct morphologies in vitro, J. Biol. Chem. 274 (1999) 7619–7622.
[34] L. Narhi, S.J. Wood, S. Steavenson, Y. Jiang, G.M. Wu, D. Anafi, S.A. Kaufman, F. Martin, K. Sitney, P. Denis, Both familial Parkinson's disease mutations accelerate α-synuclein aggregation, J. Biol. Chem. 274 (1999) 9843–9846.
[35] P.H. Weinreb, W. Zhen, A.W. Poon, K.A. Conway, P.T. Lansbury, NACP, a protein implicated in Alzheimer's disease and learning, is natively unfolded, Biochemistry 35 (1996) 13709–13715.
[36] A.L. Biere, S.J. Wood, J. Wypych, S. Steavenson, Y. Jiang, D. Anafi, F.W. Jacobsen, M.A. Jarosinski, G.-M. Wu, J.-C. Louis, Parkinson's disease-associated α-synuclein is more fibrillogenic than β-and γ-synuclein and cannot cross-seed its homologs, J. Biol. Chem. 275 (2000) 34574–34579.
[37] A.E. Powers, D.S. Patel, Expression and Purification of Untagged α-Synuclein, Alpha-Synuclein, Springer, 2019, pp. 261–269.
[38] J.Y. Choi, Y.M. Sung, H.J. Park, E.H. Hur, S.J. Lee, C. Hahn, B.R. Min, I.K. Kim, S. Kang, H. Rhim, Rapid purification and analysis of α-synuclein proteins: C-terminal truncation promotes the conversion of α-synuclein into a protease-sensitive form in Escherichia coli, Biotechnol. Appl. Biochem. 36 (2002) 33–40.
[39] V.N. Uversky, J. Li, A.L. Fink, Evidence for a partially folded intermediate in α-synuclein fibril formation, J. Biol. Chem. 276 (2001) 10737–10744.

[40] C. Huang, G. Ren, H. Zhou, C.-c. Wang, A new method for purification of recombinant human α-synuclein in Escherichia coli, Protein Expr. Purif. 42 (2005) 173–177.
[41] K.D. Kloepper, W.S. Woods, K.A. Winter, J.M. George, C.M. Rienstra, Preparation of α-synuclein fibrils for solid-state NMR: expression, purification, and incubation of wild-type and mutant forms, Protein Expr. Purif. 48 (2006) 112–117.
[42] L. Caldinelli, D. Albani, L. Pollegioni, One single method to produce native and Tat-fused recombinant human α-synuclein in Escherichia coli, BMC Biotechnol. 13 (2013) 32.
[43] H.R. Gerding, C. Karreman, A. Daiber, J. Delp, D. Hammler, M. Mex, S. Schildknecht, M. Leist, Reductive modification of genetically encoded 3-nitro-tyrosine sites in alpha synuclein expressed in E. coli, Redox biology 26 (2019) 101251.
[44] W.S. Davidson, A. Jonas, D.F. Clayton, J.M. George, Stabilization of α-synuclein secondary structure upon binding to synthetic membranes, J. Biol. Chem. 273 (1998) 9443–9449.
[45] E.S. Luth, T. Bartels, U. Dettmer, N.C. Kim, D.J. Selkoe, Purification of α-synuclein from human brain reveals an instability of endogenous multimers as the protein approaches purity, Biochemistry 54 (2014) 279–292.
[46] T. Bartels, J.G. Choi, D.J. Selkoe, α-Synuclein occurs physiologically as a helically folded tetramer that resists aggregation, Nature 477 (2011) 107.
[47] M. Karampetsou, M.T. Ardah, M. Semitekolou, A. Polissidis, M. Samiotaki, M. Kalomoiri, N. Majbour, G. Xanthou, O.M. El-Agnaf, K. Vekrellis, Phosphorylated exogenous alpha-synuclein fibrils exacerbate pathology and induce neuronal dysfunction in mice, Sci. Rep. 7 (2017) 16533.
[48] C.E.-H. Moussa, C. Wersinger, M. Rusnak, Y. Tomita, A. Sidhu, Abnormal migration of human wild-type α-synuclein upon gel electrophoresis, Neurosci. Lett. 371 (2004) 239–243.
[49] E.I. Yakupova, L.G. Bobyleva, I.M. Vikhlyantsev, A.G. Bobylev, Congo Red and amyloids: history and relationship, Biosci. Rep. 39 (2019).
[50] P. Frid, S.V. Anisimov, N. Popovic, Congo red and protein aggregation in neurodegenerative diseases, Brain Res. Rev. 53 (2007) 135–160.
[51] C. Xue, T.Y. Lin, D. Chang, Z. Guo, Thioflavin T as an amyloid dye: fibril quantification, optimal concentration and effect on aggregation, Royal Society open science 4 (2017) 160696.
[52] G. Semisotnov, N. Rodionova, O. Razgulyaev, V. Uversky, A. Gripas, R. Gilmanshin, Study of the “molten globule” intermediate state in protein folding by a hydrophobic fluorescent probe, Biopolymers: Original Research on Biomolecules 31 (1991) 119–128.